Supplement of Atmos. Chem. Phys., 18, 13197–13214, 2018
https://doi.org/10.5194/acp-18-13197-2018-supplement

Atmospheric Chemistry and Physics
Open Access
EGU

Supplement of

Molecular insights on aging and aqueous-phase processing from ambient biomass burning emissions-influenced Po Valley fog and aerosol

Matthew Brege et al.

Correspondence to: Lynn R. Mazzoleni (lrmazzol@mtu.edu)

Table of Contents

1. FT-ICR MS data processing and molecular formula assignment review

The individual transient scans of FT-ICR MS data for each sample were reviewed manually and the unacceptable scans with an abrupt change in the total ion current were removed; the remaining transient scans were co-added together to create the working file for each sample (this helped to increase signal to noise and enhance sensitivity). Molecular formula assignments were made as previously described (Mazzoleni et al., 2010; Putman et al., 2012; Zhao et al., 2013; Dzepina et al., 2015) using Sierra Analytics Composer software (version 1.0.5) within the limits of: $C_{2\text{-}200}H_{4\text{-}1000}O_{1\text{-}20}N_{0\text{-}3}S_{0\text{-}1}$. Masses were calculated from measured *m/z* values, assuming an ion charge of -1 from the electrospray. The calculator uses a CH_2 Kendrick mass defect (KMD) analysis to sort homologous ion series and extend the molecular formula assignments to higher masses (Hughey et al., 2001; Kujawinski and Behn, 2006). A de novo cut-off at *m/z* 500 was applied, indicating that no new formula assignments would occur above *m/z* 500, unless the formula was part of an existing CH_2 homologous series that began at a point lower than *m/z* 500. This is necessary because the number of possible molecular formulas increases at higher values. The minimum relative abundance required for molecular formula assignment was > 10 times the estimated signal-to-noise ratio, determined for each sample between *m/z* 900–1000. Only integer values up to 40 were allowed for the double bond equivalents (DBE). The data set was manually reviewed to remove: formulas with an absolute error > 3 ppm, elemental ratios that were not chemically sensible (such as O:C > 3 or H:C < 0.3), and formulas which violated the rule of 13 or violated the nitrogen rule. The rule of 13 checks for a reasonable number of heteroatoms in a formula. A base formula (C_nH_{n+r}) can be generated for any measured mass by solving: $\frac{M}{13} = n + \frac{r}{13}$ (Pavia, 2009). Then, the maximum number of "large atoms" (C, O, N, S) in a formula is defined as the mass divided by 13, because substituting for a heteroatom (O, N or S) involves a substitution for at least one carbon. This maximum number is then compared to the actual number of "large atoms" in a formula, and those formulas exceeding the maximum number are rejected. The nitrogen rule removes formulas with odd masses that do not contain an odd number of nitrogen atoms, and even masses that do not contain an even number (or no) nitrogen atoms; this is due to the odd numbered valence of nitrogen (Pavia, 2009). Molecular formulas that contained ^{13}C or ^{34}S were also removed from the data set. Homologous series with large gaps in the DBE trend were removed, as well as homologous series with a length of one. The assigned formulas were also analyzed with consideration to the DBE and oxygen number trends, (Herzsprung et al., 2014) where unreliable formula assignments were also removed.

2. Ultrahigh resolution FT-ICR MS results

The total ion abundance of the identified monoisotopic molecular formulas reported for each sample was determined by their summation. Then, these values were used to normalize the individual ion abundances within each sample using a ratio of the individual ion intensity to this total ion abundance. Then, the values were rescaled using a normalization constant (10,000). This normalization procedure was done to remove analytical biases introduced by trace contaminants with high electrospray efficiency.

Reconstructed difference mass spectra of the assigned molecular formulas for both fog and aerosol samples are shown in Fig. S3. These difference mass spectra permit a direct comparison of the samples using normalized

relative abundances. The individual relative abundances were normalized by the total abundance of the assigned molecular formulas identified in each of the samples. In Fig. S3, the individual masses with higher abundances in either the positive or negative direction were substantially greater in one of the two samples, whereas the masses of similar abundance tended to cancel each other. To enhance the interpretation of the compositional differences, the individual masses were color-coded to represent the number of oxygen atoms in the assigned formula. Overall, we observed higher numbers of oxygen in the masses of the two samples with aged biomass burning emissions influence compared to the two samples with fresh biomass burning emissions influence. The molecular formulas assigned to the fresh samples had approximately 0-5 oxygen atoms over the mass range of 50-250 Da, 5-10 oxygen atoms over 250-550 Da, and a few molecular formulas were assigned with 10-15 oxygen atoms over 500-600 Da. In contrast, the aged samples had a large number of molecular formulas with 10-15 oxygen atoms in the range of 400-550 Da. This clearly shows a greater amount of oxidation in the aged influenced samples compared to the fresh influenced samples.

KMD diagrams can be used as useful tools to visualize the relationships between the many molecular formulas of complex mixtures such as atmospheric samples. We used Kendrick mass defect to sort the molecular formulas into CH_2 homologous series of identical heteroatom content and DBE, where the formulas in the same series differ only by a number of CH_2 units (Stenson et al., 2003). It should be noted that the presence of multiple formulas in the same homologous series does not necessarily imply a related chemical structure. The homologous series are visible as horizontal rows of formulas in Figs. S6 and S7. There were multiple homologous series per subclass, where the base formula for each series differ in DBE and increase in KMD to form an ensemble of "steps" within each subclass. In our samples individual CHO and CHNO subclasses had approximately 5-16 different homologous series, while CHOS and CHNOS subclasses had approximately 3-10 different homologous series. The number of homologous series in a subclass increased with oxygen number, and peaked near the median oxygen number, then decreased again towards the maximum number of oxygen; this led to fewer molecular formulas in subclasses with higher and lower oxygen numbers, and more formulas in subclasses near the median oxygen number. The subclasses with the highest numbers of molecular formulas per elemental group were: O_7, NO_8, O_7S and NO_9S. It was atypical for the unique formulas of a sample to be completely unrelated to other formulas across the data set; often the unique formulas were extensions of homologous series that appeared across samples.

3. FT-ICR MS data set

An abbreviated list of the complete FT-ICR MS dataset is provided and is available on Digital Commons: http://digitalcommons.mtu.edu/chemistry-fp/98/

4. Supplemental Figures and tables

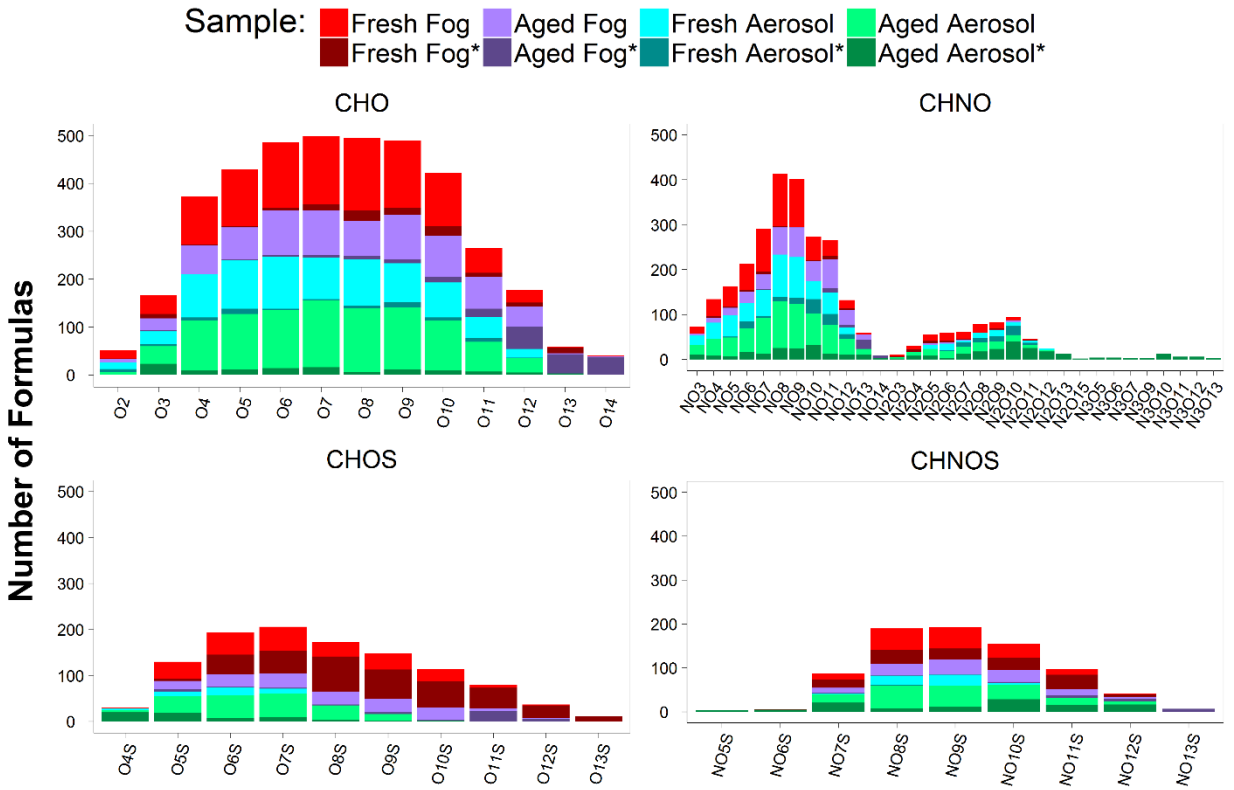

Figure S1: Distributions of the molecular formulas within all 64 elemental group subclasses for CHO, CHNO, CHOS and CHNOS groups as indicated in the Figure. The total number of molecular formulas for each SPE-recovered WSOC sample were split into two groups of unique and non-unique formulas; the darker shade represents formulas unique to a sample, (denoted in the Figure legend with an asterisk after the sample name, e.g. "Fresh Fog*") while the lighter shade represents common formulas. The sample names Fresh Fog, Aged Fog, Fresh Aerosol, and Aged Aerosol correspond to SPC0106F, SPC0201F, BO0204N, and BO0213D, respectively.

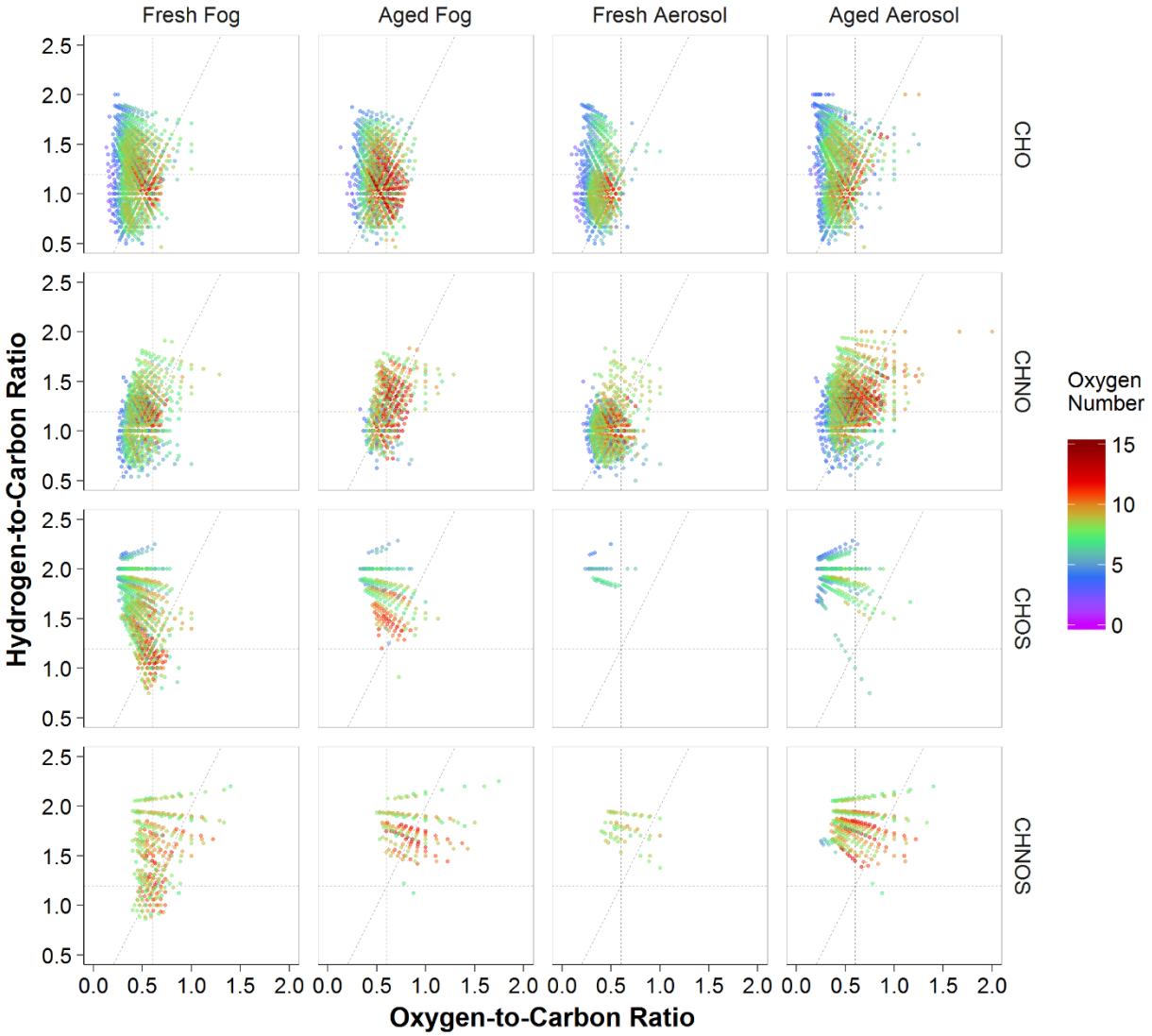

Figure S2: van Krevelen diagrams for the SPE-recovered WSOC by elemental group (rows) and sample (columns) as indicated in the Figure. Dashed lines represent H:C = 1.2 (horizontal), O:C = 0.6 (vertical) and OS_C = 0 (diagonal) as described in Tu et al. (2016). Formulas are color scaled to the number of oxygen atoms in the assigned formula. The sample names Fresh Fog, Aged Fog, Fresh Aerosol, and Aged Aerosol correspond to SPC0106F, SPC0201F, BO0204N, and BO0213D, respectively.

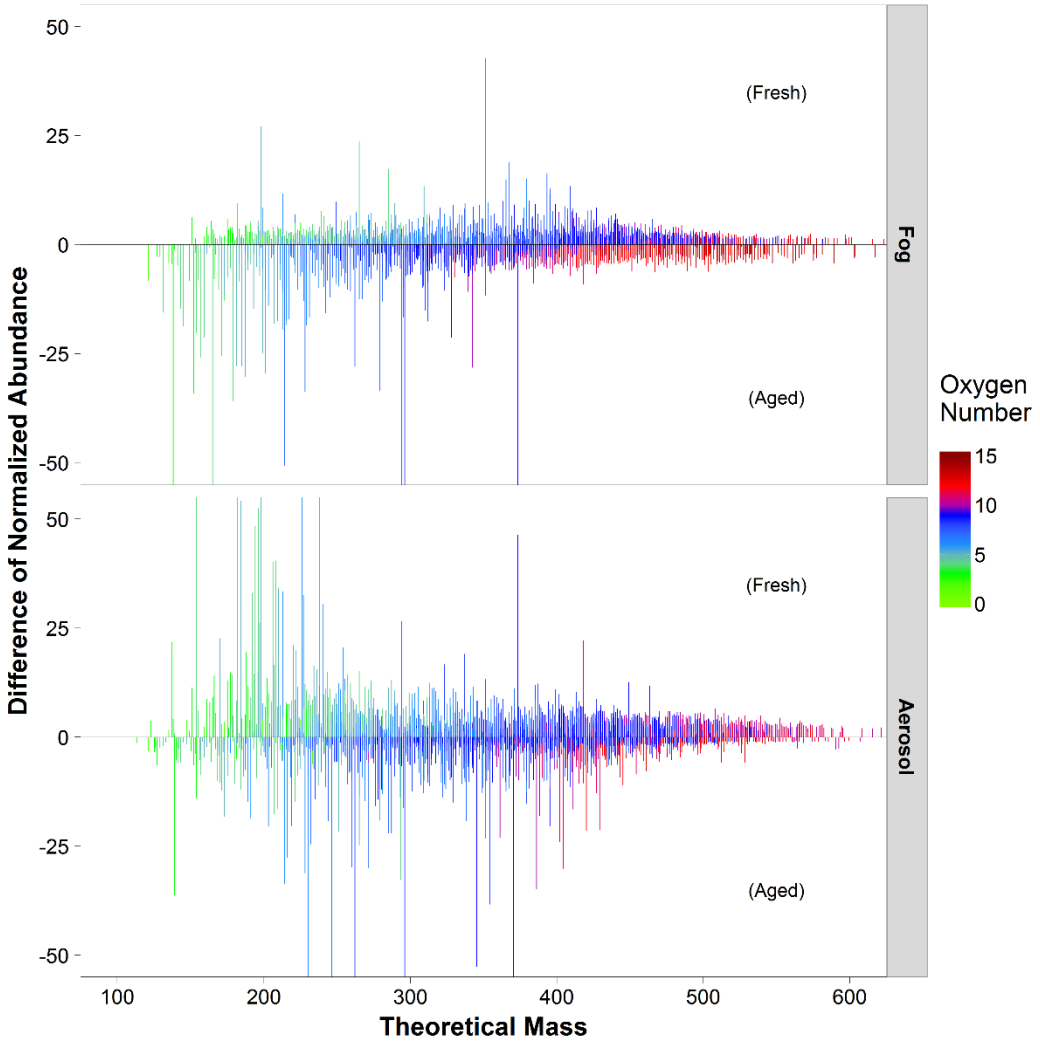

Figure S3: Reconstructed difference mass spectra for theoretical masses of assigned molecular formulas in the Po Valley samples with normalized relative abundance. Fresh influenced samples (SPC0106F and BO0204N) are plotted with positive abundance and aged influenced samples (SPC0201F and BO0213D) are plotted with negative abundance. Molecular compositions in both samples with the same mass and similar normalized relative abundance are reduced toward zero. The peaks in the mass spectra are color scaled to the number of oxygen atoms in the assigned molecular formula, where it can be observed that the aged samples shift towards species with higher oxygen numbers at lower masses, compared to the fresh samples. The sample names Fresh Fog, Aged Fog, Fresh Aerosol, and Aged Aerosol correspond to SPC0106F, SPC0201F, BO0204N, and BO0213D, respectively.

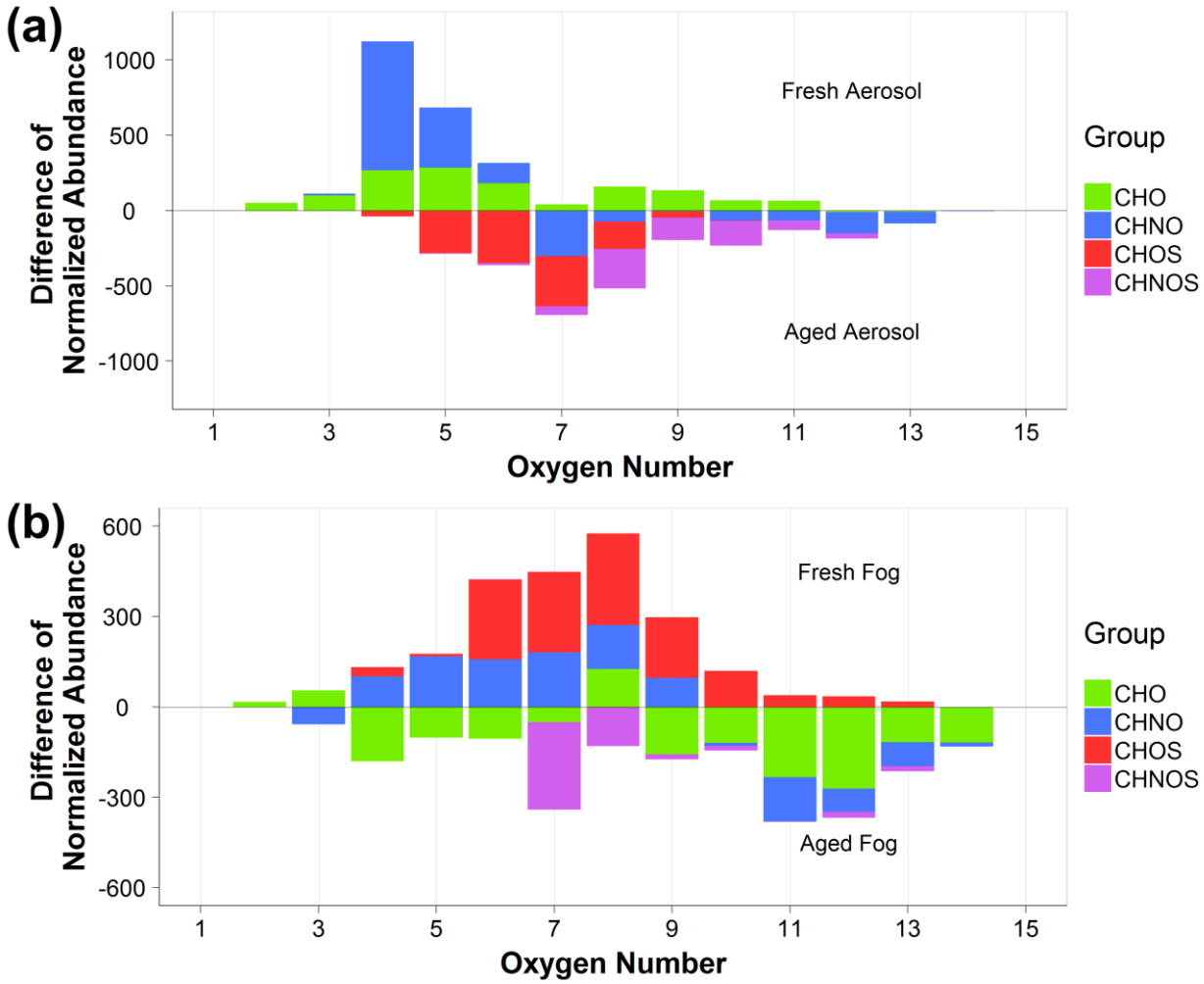

Figure S4: Oxygen difference trends for aerosol (a) and fog (b) samples. Abundance trends were calculated as in Figure 6 of the main text, and then the respective aged sample normalized abundance was subtracted from the fresh sample normalized abundance for each oxygen number value. A positive difference of abundance indicates an enhanced abundance of formulas in the fresh sample compared to the aged sample. Similarly, a negative difference of abundance indicates an enhanced abundance of formulas in the aged sample compared to the fresh sample. The sample names Fresh Fog, Aged Fog, Fresh Aerosol, and Aged Aerosol correspond to SPC0106F, SPC0201F, BO0204N, and BO0213D, respectively.

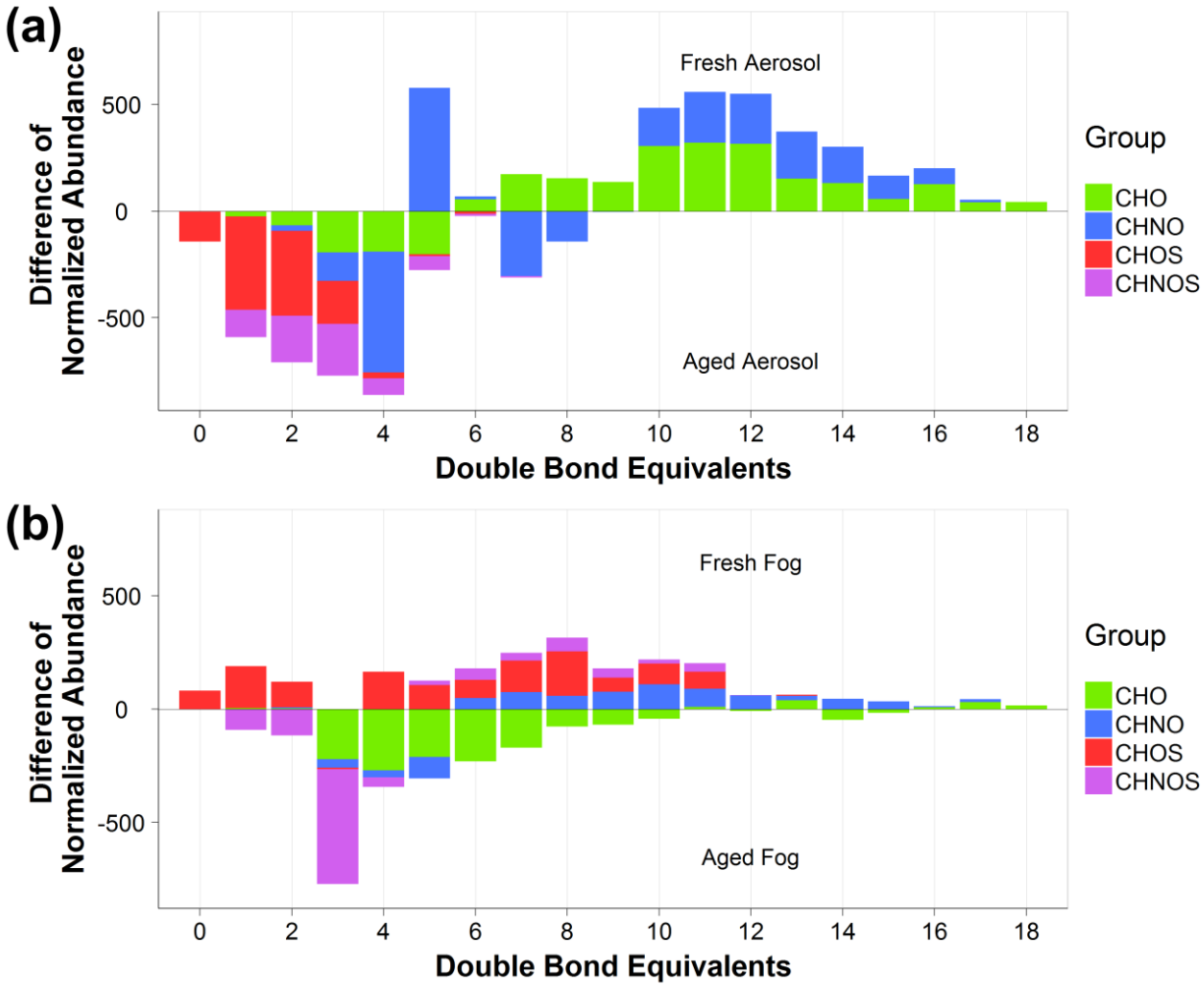

Figure S5: Double bond equivalent difference trends for aerosol (a) and fog (b) samples. Abundance trends were calculated as in Figure 6 of the main text, and then the respective aged sample normalized abundance was subtracted from the fresh sample normalized abundance for each integer double bond equivalent value. A positive difference of abundance indicates an enhanced abundance of formulas in the fresh sample compared to the aged sample. Similarly, a negative difference of abundance indicates an enhanced abundance of formulas in the aged sample compared to the fresh sample. The sample names Fresh Fog, Aged Fog, Fresh Aerosol, and Aged Aerosol correspond to SPC0106F, SPC0201F, BO0204N, and BO0213D, respectively.

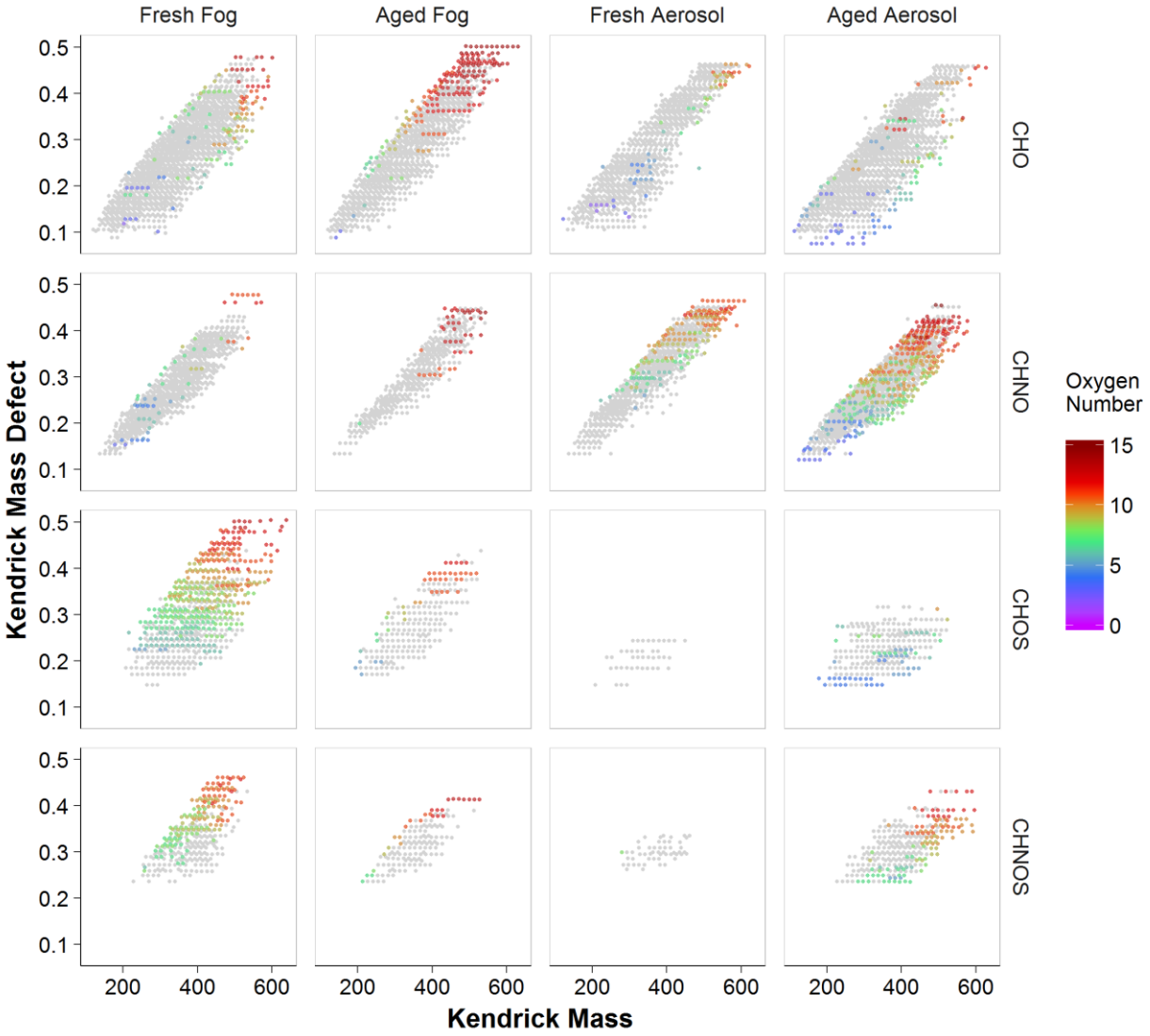

Figure S6: Kendrick mass defect diagrams for each of the Po Valley samples, partitioned by elemental group (rows) and sample (columns) as indicated in the Figure. The molecular formulas unique to each sample are color scaled to the number of oxygen atoms in the assigned formula; grey points represent formulas which are common. Homologous series of molecular formulas are visible as horizontal rows of points, where formulas which are unique to a sample may make up all or only part of an individual homologous series. The sample names Fresh Fog, Aged Fog, Fresh Aerosol, and Aged Aerosol correspond to SPC0106F, SPC0201F, BO0204N, and BO0213D, respectively.

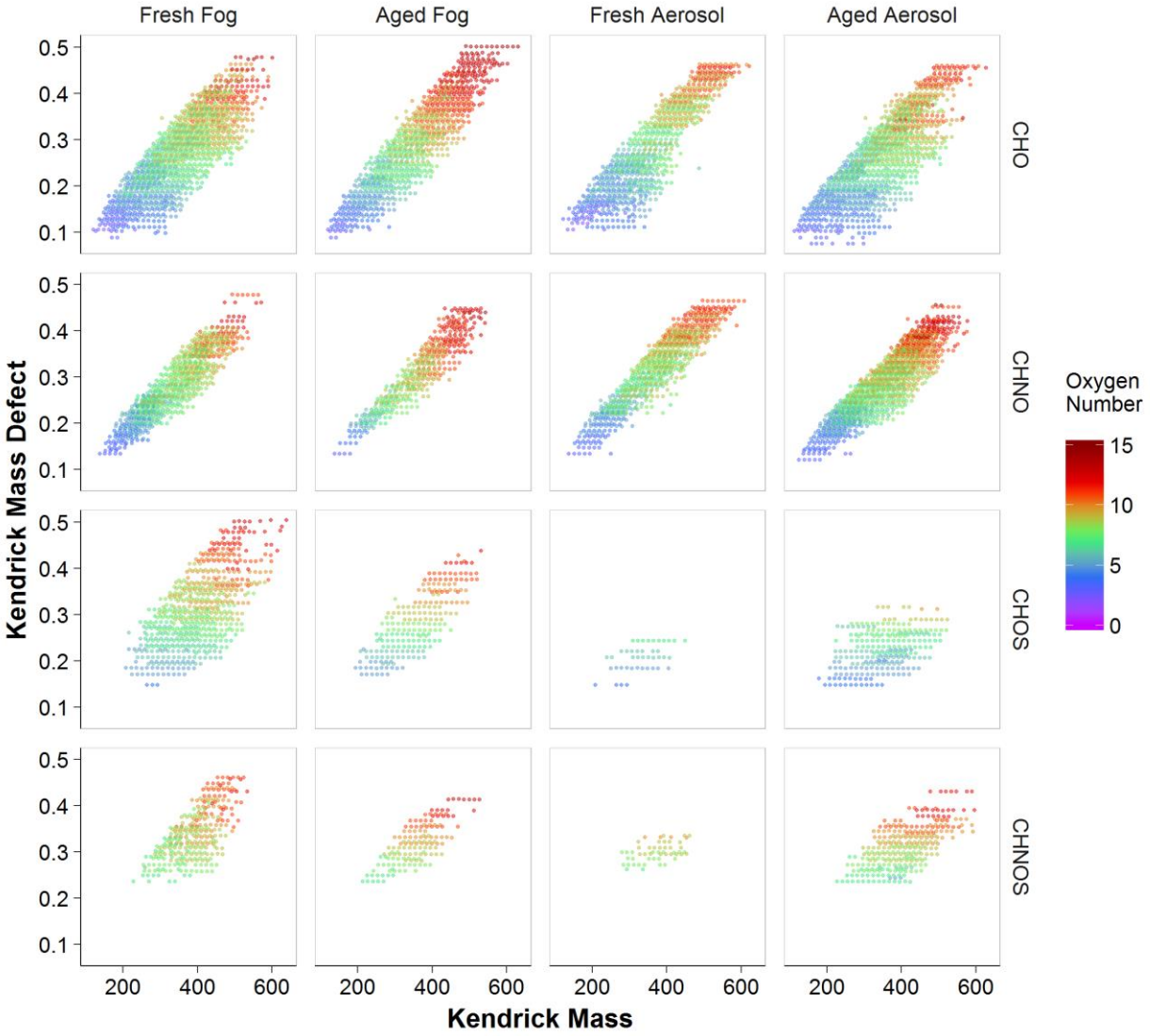

Figure S7: Kendrick mass defect diagrams for each of the Po Valley samples, partitioned by elemental group (rows) and sample (columns) as indicated in the Figure. Molecular formulas are color scaled to the number of oxygen atoms in the assigned formula. The sample names Fresh Fog, Aged Fog, Fresh Aerosol, and Aged Aerosol correspond to SPC0106F, SPC0201F, BO0204N, and BO0213D, respectively.

Table S1: Summary of the literature structural insights associated with the identified molecular formulas observed in this study. Because the identified molecular formulas may represent a variety of structural isomers, we note that matched molecular formulas do not necessarily correspond to the same molecular structure or atmospheric origin. The normalized abundances are indicated for each sample, where "ND" (not detected), "Low" (≤ 3%), "Med", (> 3% and ≤ 15%), "High" (> 15% and ≤ 50%) and "Very High" (> 50%). Molecular formulas from the literature are provided with their references.

Formula	SPC0106F	SPC0201F	BO0204N	BO0213D	Possible Identity	Reference*
$C_4H_6O_5$	ND	ND	ND	Low	syringol aqSOA	A
$C_5H_6O_3$	ND	ND	ND	Low	ambient cloud water	B
$C_5H_6O_4$	ND	Low	ND	Low	syringol aqSOA	A, B
$C_5H_6O_5$	ND	ND	ND	Low	syringol aqSOA (ketoglutaric acid)	A, C-E
$C_5H_8O_4$	ND	Med	ND	Low	ambient cloud water (methylsuccinic acid and glutatric acid)	B-F
$C_5H_8O_5$	ND	ND	ND	Low	ambient cloud water (hydroxyglutaric acid)	B, G
$C_6H_4N_2O_5$	High	Med	Low	Low	dinitrophenol	H
$C_6H_5NO_3$	High	High	Med	Med	nitrophenol	B, H
$C_6H_5NO_4$	High	High	Very High	Med	nitrocatechol	B, H
$C_6H_5NO_5$	ND	ND	Med	Low	ambient cloud water	B
$C_6H_6O_3$	ND	ND	ND	Low	pyrogallol	C-E
$C_6H_6O_4$	ND	Low	ND	Med	phenol SOA	
$C_6H_6O_5$	ND	ND	ND	Low	syringol aqSOA	A
$C_6H_8O_4$	Low	Med	ND	Med	ambient cloud water	B
$C_6H_8O_6$	ND	ND	ND	Low	syringol aqSOA	A
$C_6H_{10}O_3$	ND	Low	ND	Low	ambient cloud water	B
$C_6H_{10}O_4$	ND	Med	ND	Low	ambient cloud water (methylglutaric acid and adipic acid)	B-F
$C_6H_{10}O_5$	ND	Low	ND	Low	levoglucosan	B-F, I
$C_6H_{10}O_6$	ND	ND	ND	Low	dimethyltartaric acid	J
$C_7H_5NO_5$	High	Med	Med	Med	nitrosalicylic acid	H
$C_7H_6O_2$	Med	Med	ND	Low	ambient cloud water (benzoic acid)	B, F
$C_7H_6O_3$	Med	Med	Med	Med	phenol aqSOA (dihydroxybenzaldehyde and hydroxybenzoic acid)	A, C-E
$C_7H_6O_4$	Med	Low	Low	Med	phenol aqSOA	A

Formula	SPC0106F	SPC0201F	BO0204N	BO0213D	Possible Identity	Reference*
$C_7H_6O_5$	ND	Low	ND	Low	syringol aqSOA	K
$C_7H_6N_2O_5$	Med	Med	Med	Low	ambient cloud water	B, L
$C_7H_6N_2O_6$	Med	ND	Med	Low	ambient cloud water	B, L
$C_7H_7NO_3$	High	High	Med	High	methyl-nitrophenol	B, H
$C_7H_7NO_4$	High	Med	Med	Med	ambient cloud water (nitroguaiacol and methyl-nitrocatechol)	B,H
$C_7H_7NO_5$	Med	Low	Med	Med	ambient cloud water	B
$C_7H_8O_3$	Med	Low	ND	High	guaiacol SOA	
$C_7H_8O_4$	Med	Med	Low	Low	guaiacol SOA	
$C_7H_8O_5$	Low	Med	Low	Med	guaiacol SOA	
$C_7H_8O_6$	Low	Low	ND	Med	guaiacol SOA	
$C_7H_{10}O_4$	Low	Med	Low	Med	ambient cloud water	L
$C_7H_{10}O_6$	Low	Low	Low	Med	guaiacol aqSOA	A
$C_7H_{12}O_4$	ND	Med	ND	Low	ambient cloud water (pimelic acid)	C-E, L
$C_7H_{12}O_5$	ND	Low	Low	Med	biogenic SOA (hydroxy-dimethylglutaric acid)	G
$C_7H_{12}O_6S$	ND	Low	ND	Low	ambient cloud water	L
$C_7H_{12}O_7$	Low	ND	ND	ND	syringol aqSOA	A
$C_7H_{14}O_5S$	Low	Med	ND	Low	dodecane aqSOA	L
$C_7H_{14}O_6S$	ND	Low	ND	Low	ambient cloud water	L
$C_8H_5NO_4$	Med	Low	Med	Low	ambient cloud water	B
$C_8H_6O_3$	Med	Med	Low	Low	ambient cloud water and guaiacol aqSOA	A, B
$C_8H_6O_4$	Med	Very High	Low	Low	ambient cloud water (phthalic acid)	B-F
$C_8H_6O_5$	Med	Med	ND	Low	phenol aqSOA	A
$C_8H_7NO_3$	Med	ND	Med	High	ambient cloud water	B
$C_8H_7NO_4$	Med	Med	Med	High	ambient cloud water	B
$C_8H_7NO_5$	High	Med	Med	High	ambient cloud water	B
$C_8H_8O_2$	Med	Med	Low	Low	ambient cloud water (o-toluic acid)	B, F
$C_8H_8O_3$	High	Med	Med	Low	ambient cloud water (vanillin)	B-E

Formula	SPC0106F	SPC0201F	BO0204N	BO0213D	Possible Identity	Reference*
$C_8H_8O_4$	Med	Med	Low	Low	vanillic acid	C-F, I
$C_8H_9NO_3$	Med	Med	Med	Low	ambient cloud water	B
$C_8H_9NO_4$	High	Med	Very High	High	ambient cloud water	B
$C_8H_9NO_5$	High	Med	High	High	ambient cloud water	B
$C_8H_{10}O_3$	Med	Low	ND	Low	syringol	A,F, I, K
$C_8H_{10}O_4$	Low	Med	ND	Low	syringol SOA	
$C_8H_{10}O_5$	Med	Med	Low	Med	syringol aqSOA	K-L
$C_8H_{10}O_6$	Low	Med	Low	Med	syringol aqSOA	A
$C_8H_{10}O_7$	ND	Low	ND	Low	syringol aqSOA	A
$C_8H_{12}O_6$	Med	Med	Low	Med	biogenic SOA (methyl-butanetricarboxylic acid)	G
$C_8H_{12}O_7S$	ND	Low	ND	ND	ambient cloud water	L
$C_8H_{12}O_8S$	Med	Low	ND	Low	ambient cloud water	L
$C_8H_{14}O_6S$	Low	Med	ND	Low	ambient cloud water	L
$C_8H_{14}O_7$	Med	ND	ND	ND	methylglyceric acid dimer	J
$C_8H_{14}O_7S$	ND	Low	ND	ND	ambient cloud water	L
$C_8H_{16}O_6S$	Med	Med	Low	Med	ambient cloud water	M
$C_9H_7NO_4$	Med	Low	Med	Low	ambient cloud water	B
$C_9H_8O_2$	Med	Low	Low	ND	ambient cloud water	B
$C_9H_8O_3$	Med	Med	Med	Med	ambient cloud water (coumaryc acid)	B-E
$C_9H_8N_2O_6$	Low	ND	Low	Med	ambient cloud water	L
$C_9H_9NO_3$	Med	ND	Low	Med	ambient cloud water	B
$C_9H_9NO_3$	Med	ND	Low	Med	laboratory brown carbon aqSOA	N
$C_9H_9NO_4$	Med	Low	Med	Med	ambient cloud water	B
$C_9H_{10}O_3$	Med	Low	Low	Low	laboratory brown carbon aqSOA (acetovanillone and dimethoxybenzaldehyde)	A, C-F, K, O
$C_9H_{10}O_4$	Med	Med	Low	Low	syringol aqSOA (syringaldehyde)	C-F, I, K
$C_9H_{10}O_5$	Med	Med	Low	Low	syringic acid	C-F, I
$C_9H_{11}NO_3$	Med	Low	Low	Med	tyrosine	

Formula	SPC0106F	SPC0201F	BO0204N	BO0213D	Possible Identity	Reference*
$C_9H_{11}NO_4$	Med	Low	Med	Med	ambient cloud water	B
$C_9H_{12}O_3$	Low	Low	ND	Low	methylsyringol	F
$C_9H_{12}O_5$	Med	Med	Low	Low	ambient cloud water	L
$C_9H_{12}O_7S$	Low	ND	ND	ND	ambient cloud water	L
$C_9H_{12}N_2O_3$	ND	ND	ND	Low	laboratory brown carbon aqSOA	O
$C_9H_{12}N_2O_3$	ND	ND	ND	Low	laboratory brown carbon aqSOA	N
$C_9H_{13}NO_5$	Low	ND	ND	Med	laboratory brown carbon aqSOA	N
$C_9H_{14}O_3$	Low	Low	ND	Low	ketolimononaldehyde	P
$C_9H_{14}O_4$	Med	Med	ND	Low	biogenic SOA (pinic acid)	G
$C_9H_{14}O_6S$	Med	ND	ND	ND	ambient cloud water	L
$C_9H_{14}O_7S$	Low	Med	ND	Low	ambient cloud water	L
$C_9H_{14}O_8S$	Med	Med	ND	Low	ambient cloud water	L
$C_9H_{14}O_9S$	Low	Low	ND	ND	ambient cloud water	L
$C_9H_{15}NO_8S$	Very High	Very High	Low	Very High	ambient cloud water	L
$C_9H_{16}O_4$	High	Med	Low	Low	azelaic acid	C-F
$C_9H_{16}O_6S$	Med	Med	ND	Med	ambient cloud water	L
$C_9H_{16}O_7S$	Low	Med	ND	Low	ambient cloud water	L
$C_9H_{16}O_8S$	ND	Low	ND	ND	ambient cloud water	L
$C_9H_{18}O_6S$	Med	Med	Low	Med	ambient cloud water, marine SOA	I, M
$C_9H_{18}O_8S$	ND	ND	ND	Low	ambient cloud water	M
$C_{10}H_8O_3$	Med	Low	Med	Low	syringol aqSOA	A
$C_{10}H_{10}O_4$	High	Med	Med	ND	ferrulic acid	C-E
$C_{10}H_{12}O_2$	Low	Low	ND	Low	eugenol	F
$C_{10}H_{12}O_4$	Med	Low	Low	Low	acetosyringone	C-E
$C_{10}H_{14}O_3$	Low	Low	ND	Low	ketopinic acid	G
$C_{10}H_{14}O_5$	Med	Med	Low	Low	ambient cloud water	L
$C_{10}H_{14}O_6$	Med	Med	ND	Low	ambient cloud water	L
$C_{10}H_{14}O_7S$	Med	ND	ND	ND	ambient cloud water	L
$C_{10}H_{14}O_8S$	Low	Low	ND	ND	ambient cloud water	L
$C_{10}H_{16}O_3$	Low	Low	ND	Low	pinonic acid	C-E, G

Formula	SPC0106F	SPC0201F	BO0204N	BO0213D	Possible Identity	Reference*
$C_{10}H_{16}O_6S$	Med	ND	ND	ND	ambient cloud water	L
$C_{10}H_{16}O_7S$	Med	High	ND	Low	ambient cloud water	L
$C_{10}H_{16}O_8S$	ND	Med	ND	Low	ambient cloud water	L
$C_{10}H_{16}O_9S$	Low	Low	ND	ND	ambient cloud water	L
$C_{10}H_{17}NO_7S$	Very High	Very High	High	Very High	ambient cloud water	L
$C_{10}H_{17}NO_{10}S$	Med	Med	Low	Med	ambient cloud water	L
$C_{10}H_{18}O_5S$	ND	Med	ND	ND	ambient cloud water	L
$C_{10}H_{18}O_7S$	Med	Med	ND	Low	ambient cloud water	L
$C_{10}H_{18}O_8S$	Low	Med	ND	ND	ambient cloud water	L
$C_{10}H_{19}NO_9S$	High	Med	Low	Med	ambient cloud water	M
$C_{10}H_{20}O_5S$	Med	Med	Low	High	ambient cloud water	M
$C_{10}H_{20}O_6S$	Med	Med	ND	Med	marine SOA	I
$C_{10}H_{20}O_7S$	Low	Low	ND	Low	ambient cloud water	L
$C_{11}H_{10}O_8$	ND	Low	ND	ND	phenol aqSOA	A
$C_{11}H_{21}NO_9S$	Med	Med	Low	Med	ambient cloud water	M
$C_{11}H_{22}O_5S$	Med	Med	Low	High	ambient cloud water	M
$C_{11}H_{22}O_6S$	Med	Med	ND	Med	marine SOA	I
$C_{12}H_{10}O_2$	Low	ND	Low	ND	phenol aqSOA	A, K
$C_{12}H_{10}O_3$	Low	ND	Low	Low	phenol aqSOA	A
$C_{12}H_{10}O_4$	ND	ND	Low	Low	phenol aqSOA	A
$C_{12}H_{10}O_7$	Med	Med	Low	Low	syringol aqSOA	K
$C_{12}H_{10}N_2O_8$	ND	ND	Low	ND	ambient cloud water	B
$C_{12}H_{11}NO_4$	Med	ND	Low	Low	laboratory brown carbon aqSOA	N
$C_{12}H_{12}O_6$	Med	Med	Low	Low	syringol aqSOA	K, L
$C_{12}H_{12}O_7$	Med	Med	Low	Low	syringol aqSOA	A, K, L
$C_{12}H_{14}O_4$	Med	Low	Low	Med	syringol aqSOA	A
$C_{12}H_{14}N_2O_4$	ND	ND	ND	Low	laboratory brown carbon aqSOA	O
$C_{12}H_{14}N_2O_4$	ND	ND	ND	Low	laboratory brown carbon aqSOA	N
$C_{12}H_{16}N_2O_5$	ND	ND	ND	Low	laboratory brown carbon aqSOA	O
$C_{12}H_{17}NO_7$	Low	Low	Low	Low	laboratory brown carbon aqSOA	N

Formula	SPC0106F	SPC0201F	BO0204N	BO0213D	Possible Identity	Reference*
$C_{12}H_{20}O_7S$	Med	Med	ND	Med	ambient cloud water	L
$C_{12}H_{22}O_7S$	Med	Med	Low	Med	ambient cloud water	M
$C_{12}H_{23}NO_9S$	Med	Med	Low	Med	ambient cloud water	M
$C_{12}H_{24}O_5S$	Med	Low	Low	High	ambient cloud water	M
$C_{12}H_{24}O_6S$	Med	Med	ND	Med	marine SOA	I
$C_{12}H_{26}O_4S$	High	ND	Med	Low	ambient cloud water	M
$C_{13}H_{10}O_3$	ND	ND	ND	Low	guaiacol aqSOA	A
$C_{13}H_{10}O_4$	Med	Low	Low	ND	guaiacol aqSOA	A
$C_{13}H_{10}O_5$	Med	ND	Low	Low	guaiacol aqSOA	A
$C_{13}H_{12}O_4$	ND	ND	Low	Low	guaiacol aqSOA	A
$C_{13}H_{12}O_6$	Med	Med	Low	Low	guaiacol aqSOA	A, L
$C_{13}H_{14}O_5$	Med	Med	Med	Med	syringol aqSOA	A
$C_{13}H_{14}O_7$	Med	Med	Low	Low	syringol aqSOA	A
$C_{13}H_{16}O_8$	Med	ND	Low	ND	syringol aqSOA	A
$C_{13}H_{24}O_7S$	Med	Med	Low	Med	ambient cloud water	M
$C_{13}H_{26}O_6S$	Med	Low	Low	Med	ambient cloud water, marine SOA	I, M
$C_{14}H_{10}O_5$	Med	Low	Low	Low	phenol aqSOA	A
$C_{14}H_{12}O_6$	Med	Low	Low	Low	guaiacol aqSOA	A, L
$C_{14}H_{12}O_7$	Med	Med	ND	Low	syringol aqSOA	A
$C_{14}H_{14}O_4$	ND	ND	Med	Low	guaiacol aqSOA	A, I, K
$C_{14}H_{14}O_5$	Med	Low	Low	Med	guaiacol aqSOA	A, K, L
$C_{14}H_{14}O_6$	Med	Med	Low	Med	syringol aqSOA and guaiacol aqSOA	A, K
$C_{14}H_{14}O_8$	Med	Med	ND	Low	Syringol aqSOA	A
$C_{14}H_{16}O_8$	Med	Med	Low	Low	syringol aqSOA	A
$C_{14}H_{16}O_9$	Med	Low	ND	Low	syringol aqSOA	A
$C_{14}H_{16}O_{10}$	Low	Low	ND	Low	syringol aqSOA	A
$C_{14}H_{20}O_9$	Low	Low	ND	Med	ambient cloud water	L
$C_{14}H_{24}O_8$	ND	Low	ND	ND	ambient cloud water	L
$C_{14}H_{27}NO_9S$	Med	Low	Low	Med	ambient cloud water	M
$C_{14}H_{28}O_5S$	Med	Low	Low	Med	ambient cloud water	M
$C_{14}H_{28}O_6S$	Med	Low	Low	Med	ambient cloud water	M
$C_{14}H_{30}O_4S$	Med	ND	Low	Med	ambient cloud water	M
$C_{15}H_{14}O_6$	Med	Low	Low	Low	syringol aqSOA	K, L
$C_{15}H_{14}O_8$	Med	Med	Low	Low	syringol aqSOA	K

Formula	SPC0106F	SPC0201F	BO0204N	BO0213D	Possible Identity	Reference*
$C_{15}H_{16}O_6$	Med	Med	Low	Low	syringol aqSOA	A, K, L
$C_{15}H_{16}O_8$	Med	Med	ND	Low	syringol aqSOA	A
$C_{15}H_{16}O_9$	Med	Med	ND	Low	syringol aqSOA	A, K, L
$C_{15}H_{18}O_7$	Med	Med	Low	Low	syringol aqSOA	A, K, L
$C_{15}H_{18}O_9$	Med	Med	Low	Low	syringol aqSOA	A
$C_{15}H_{18}O_{10}$	Low	Low	ND	Low	syringol aqSOA	A
$C_{15}H_{24}O_9$	Low	Low	ND	Low	ambient cloud water	L
$C_{15}H_{29}NO_9S$	Med	Low	Low	Med	ambient cloud water	M
$C_{15}H_{30}O_6S$	Med	Low	Low	Med	ambient cloud water	M
$C_{16}H_{18}O_6$	Med	Low	Low	ND	syringol aqSOA	A, I, K, L
$C_{16}H_{18}O_7$	Med	Med	Low	Low	syringol aqSOA	A
$C_{16}H_{18}O_9$	Med	Med	ND	Low	syringol aqSOA	K
$C_{16}H_{24}O_{11}S$	ND	Low	ND	ND	ambient cloud water	L
$C_{16}H_{31}NO_9S$	Med	Low	Low	Med	ambient cloud water	M
$C_{17}H_{33}NO_9S$	Med	Low	Low	Med	ambient cloud water	M
$C_{18}H_{12}O_5$	Low	ND	ND	Low	phenol aqSOA	A
$C_{18}H_{14}O_4$	Low	ND	Low	Low	phenol aqSOA	A
$C_{18}H_{26}O_{12}S$	ND	Low	ND	ND	ambient cloud water	L
$C_{18}H_{28}O_{11}S$	Low	Low	ND	ND	ambient cloud water	L
$C_{18}H_{38}O_6S$	Low	ND	ND	Low	ambient cloud water	M
$C_{19}H_{30}O_{12}S$	Low	ND	ND	ND	ambient cloud water	L
$C_{20}H_{14}O_6$	Low	ND	Low	ND	phenol aqSOA	A
$C_{20}H_{16}O_7$	Med	ND	Low	Low	guaiacol aqSOA	A
$C_{20}H_{18}O_6$	Med	ND	Low	Low	guaiacol aqSOA	A
$C_{20}H_{26}O_3$	Low	ND	Low	ND	oxodehydroabietic acid	F
$C_{20}H_{28}O_2$	ND	ND	Low	ND	dehydroabietic acid	F
$C_{21}H_{18}O_8$	Med	Low	Low	Low	guaiacol aqSOA	A
$C_{21}H_{20}O_6$	Low	ND	Low	Low	guaiacol aqSOA	A, K
$C_{21}H_{20}O_8$	Med	ND	Low	ND	guaiacol aqSOA	A
$C_{28}H_{26}O_8$	ND	ND	Low	Low	guaiacol aqSOA	A

*References: (A) Yu et al. (2016); (B) Desyaterik et al. (2013); (C) Pietrogrande et al. (2014a); (D) Pietrogrande et al. (2014b); (E) Pietrogrande et al. (2015); (F) Mazzoleni et al. (2007); (G) He et al. (2014); (H) Kitanovski et al. (2012); (I) Dzepina et al. (2015); (J) Herrmann et al. (2015); (K) Yu et al. (2014); (L) Cook et al. (2017); (M) Zhao et al. (2013); (N) Hawkins et al. (2018); (O) Lin et al. (2015) and (P) Nguyen et al. (2013).

References

Cook, R. D., Lin, Y. H., Peng, Z. Y., Boone, E., Chu, R. K., Dukett, J. E., Gunsch, M. J., Zhang, W. L., Tolic, N., Laskin, A., and Pratt, K. A.: Biogenic, urban, and wildfire influences on the molecular composition of dissolved organic compounds in cloud water, Atmos Chem Phys, 17, 15167-15180, 10.5194/acp-17-15167-2017, 2017.

Desyaterik, Y., Sun, Y., Shen, X. H., Lee, T. Y., Wang, X. F., Wang, T., and Collett, J. L.: Speciation of "brown" carbon in cloud water impacted by agricultural biomass burning in eastern China, J Geophys Res-Atmos, 118, 7389-7399, 2013.

Dzepina, K., Mazzoleni, C., Fialho, P., China, S., Zhang, B., Owen, R. C., Helmig, D., Hueber, J., Kumar, S., Perlinger, J. A., Kramer, L. J., Dziobak, M. P., Ampadu, M. T., Olsen, S., Wuebbles, D. J., and Mazzoleni, L. R.: Molecular characterization of free tropospheric aerosol collected at the Pico Mountain Observatory: a case study with a long-range transported biomass burning plume, Atmos Chem Phys, 15, 5047-5068, 2015.

Hawkins, L., Welsh, H., and Alexander, M.: Evidence for pyrazine-based chromophores in cloudwater mimics containing methylglyoxal and ammonium sulfate, Atmos. Chem. Phys. Discuss., 29, https://doi.org/10.5194/acp-2018-63, 2018.

He, Q. F., Ding, X., Wang, X. M., Yu, J. Z., Fu, X. X., Liu, T. Y., Zhang, Z., Xue, J., Chen, D. H., Zhong, L. J., and Donahue, N. M.: Organosulfates from Pinene and Isoprene over the Pearl River Delta, South China: Seasonal Variation and Implication in Formation Mechanisms, Environ Sci Technol, 48, 9236-9245, 2014.

Herrmann, H., Schaefer, T., Tilgner, A., Styler, S. A., Weller, C., Teich, M., and Otto, T.: Tropospheric Aqueous-Phase Chemistry: Kinetics, Mechanisms, and Its Coupling to a Changing Gas Phase, Chem Rev, 115, 4259-4334, 2015.

Herzsprung, P., Hertkorn, N., von Tumpling, W., Harir, M., Friese, K., and Schmitt-Kopplin, P.: Understanding molecular formula assignment of Fourier transform ion cyclotron resonance mass spectrometry data of natural organic matter from a chemical point of view, Anal Bioanal Chem, 406, 7977-7987, 2014.

Hughey, C. A., Hendrickson, C. L., Rodgers, R. P., Marshall, A. G., and Qian, K. N.: Kendrick mass defect spectrum: A compact visual analysis for ultrahigh-resolution broadband mass spectra, Anal Chem, 73, 4676-4681, 2001.

Kitanovski, Z., Grgic, I., Vermeylen, R., Claeys, M., and Maenhaut, W.: Liquid chromatography tandem mass spectrometry method for characterization of monoaromatic nitro-compounds in atmospheric particulate matter, J Chromatogr A, 1268, 35-43, 10.1016/j.chroma.2012.10.021, 2012.

Kujawinski, E. B., and Behn, M. D.: Automated analysis of electrospray ionization Fourier transform ion cyclotron resonance mass spectra of natural organic matter, Anal Chem, 78, 4363-4373, 2006.

Lin, P., Laskin, J., Nizkorodov, S. A., and Laskin, A.: Revealing Brown Carbon Chromophores Produced in Reactions of Methylglyoxal with Ammonium Sulfate, Environ Sci Technol, 49, 14257-14266, 10.1021/acs.est.5b03608, 2015.

Mazzoleni, L. R., Zielinska, B., and Moosmuller, H.: Emissions of levoglucosan, methoxy phenols, and organic acids from prescribed burns, laboratory combustion of wildland fuels, and residential wood combustion, Environ Sci Technol, 41, 2115-2122, 2007.

Mazzoleni, L. R., Ehrmann, B. M., Shen, X. H., Marshall, A. G., and Collett, J. L.: Water-Soluble Atmospheric Organic Matter in Fog: Exact Masses and Chemical Formula Identification by Ultrahigh-Resolution Fourier Transform Ion Cyclotron Resonance Mass Spectrometry, Environ Sci Technol, 44, 3690-3697, 2010.

Nguyen, T. B., Laskin, A., Laskin, J., and Nizkorodov, S. A.: Brown carbon formation from ketoaldehydes of biogenic monoterpenes, Faraday Discuss, 165, 473-494, 2013.

Pavia, D., Lampman, G., Kriz, G., Vyvyan, J.: Introduction to Spectroscopy, 4th ed., Brooks/Cole, Cengage Learning, 656 pp., 2009.

Pietrogrande, M. C., Bacco, D., Visentin, M., Ferrari, S., and Casali, P.: Polar organic marker compounds in atmospheric aerosol in the Po Valley during the Supersito campaigns - Part 2: Seasonal variations of sugars, Atmos Environ, 97, 215-225, 2014a.

Pietrogrande, M. C., Bacco, D., Visentin, M., Ferrari, S., and Poluzzi, V.: Polar organic marker compounds in atmospheric aerosol in the Po Valley during the Supersito campaigns - Part 1: Low molecular weight carboxylic acids in cold seasons, Atmos Environ, 86, 164-175, 2014b.

Pietrogrande, M. C., Sacco, D., Ferrari, S., Kaipainen, J., Ricciardelli, I., Riekkola, M. L., Trentini, A., and Visentin, M.: Characterization of atmospheric aerosols in the Po valley during the supersito campaigns - Part 3: Contribution of wood combustion to wintertime atmospheric aerosols in Emilia Romagna region (Northern Italy), Atmos Environ, 122, 291-305, 2015.

Putman, A. L., Offenberg, J. H., Fisseha, R., Kundu, S., Rahn, T. A., and Mazzoleni, L. R.: Ultrahigh-resolution FT-ICR mass spectrometry characterization of alpha-pinene ozonolysis SOA, Atmos Environ, 46, 164-172, 2012.

Stenson, A. C., Marshall, A. G., and Cooper, W. T.: Exact masses and chemical formulas of individual Suwannee River fulvic acids from ultrahigh resolution electrospray ionization Fourier transform ion cyclotron resonance mass spectra, Anal Chem, 75, 1275-1284, 2003.

Tu, P. J., Hall, W. A., and Johnston, M. V.: Characterization of Highly Oxidized Molecules in Fresh and Aged Biogenic Secondary Organic Aerosol, Anal Chem, 88, 4495-4501, 2016.

Yu, L., Smith, J., Laskin, A., Anastasio, C., Laskin, J., and Zhang, Q.: Chemical characterization of SOA formed from aqueous-phase reactions of phenols with the triplet excited state of carbonyl and hydroxyl radical, Atmos Chem Phys, 14, 13801-13816, 2014.

Yu, L., Smith, J., Laskin, A., George, K. M., Anastasio, C., Laskin, J., Dillner, A. M., and Zhang, Q.: Molecular transformations of phenolic SOA during photochemical aging in the aqueous phase: competition among oligomerization, functionalization, and fragmentation, Atmos Chem Phys, 16, 4511-4527, 2016.

Zhao, Y., Hallar, A. G., and Mazzoleni, L. R.: Atmospheric organic matter in clouds: exact masses and molecular formula identification using ultrahigh-resolution FT-ICR mass spectrometry, Atmos Chem Phys, 13, 12343-12362, 2013.